Toward High Integrity Personal Localization System Based on Informational Formalism

Mohamad Daher, Joelle Al Hage, Maan El Badaoui El Najjar, Ahmad Diab, Khalil Mohamad, François Charpillet

Towards High Integrity Personal Localization System Based on Informational Formalism

M. Daher*, J. Al Hage, M. El Badaoui El Najjar, A. Diab, M. Khalil and F. Charpillet

***Abstract*— Several computing techniques and sensor technologies have been proposed in the last two decades to provide indoor localization systems for personal in-home staying. This field known as personal localization system (PLS) is quite challenging due to some faulty sensor measurements as well as people random movements. This paper describes the ongoing work of in-home PLS using data fusion between an inertial measurement unit (IMU) and a load pressure sensing floor. In addition, a fault-tolerant fusion method is proposed using a purely informational formalism: information filter on the one hand, and information theory tools on the other hand. Residues based on the Kullback-Leibler divergence are used. Using an appropriate threshold, these residues lead to the detection and exclusion of sensors faults. The experimental results show that the proposed approach is very promising, a fault-tolerant PLS that localizes and tracks people in their home with a high accuracy.**

***Index Terms*—personal localization system; multi-sensors data fusion; sensing floor; Kalman Filter; fault-tolerant; Kullback-Leibler Divergence.**

I. INTRODUCTION

Knowing the exact position of a person at home in real time is essential to many applications like personal localization system (PLS) for elderly and disabled people during emergency situations [1,2]. Such systems actually use radio waves, magnetic fields, or other sensory information collected by different types of sensors with diverse technologies (GPS, Wi-Fi, Bluetooth, ZigBee, Ultrasounds, Infrared, etc.). These technologies vary significantly in terms of accuracy, coverage, efficiency, security, cost and power consumption, which remain important challenges in the indoor personal localization systems [3,4].

This paper presents a novel approach for PLS to locate people in their apartment in an efficient way by using wearable sensor (an IMU held by a person) and sensory equipped infrastructure (load pressure sensors under smart tiles of the INRIA Nancy - Grand Est smart apartment). The apartment is composed of a living room, bedroom, kitchen and a bathroom with a network of depth cameras and a sensing floor composed of smart tiles. Each tile (60x60cm) is equipped with four pressure sensors in the corner that are connected to a Cental Processing Unit (CPU) in the center. Tiles send data every 20 milliseconds to a processing software using ZigBee wireless technology [5]. Each tile supports a real-time process that ensures communication with its neighbors or any mediator. [6]. A schematic view of this apartment is showed in the "Fig. 1".

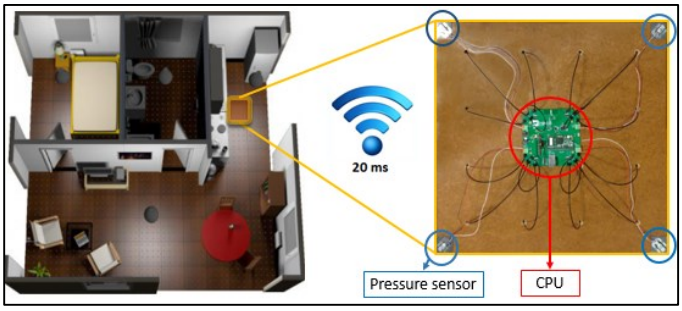

Fig. 1. At the left is the INRIA-Nancy smart apartment, at the right is the underside of a smart tile. Note that the blue circles in the corners of tiles indicate the positions of the load pressure sensors and the red circle in the center indicates the position of the CPU.

The proposed method uses an informational framework for a fault-tolerant and multi-sensor data fusion with fault detection and exclusion (FDE). The FDE method is based on a bank of extended information filter (EIF) with residual tests based on the Kullback-Leibler divergence (KLD) [7,8,9]. These residues lead to detect and exclude sensors faults by using an appropriate threshold.

II. MULTISENSORY DATA FUSION FOR POSITIONING SYSTEMS

Multi-sensor data fusion is the combination of multiple data sources to provide a robust estimation and a description of an environment. The goal is to obtain a higher integrity and

Manuscript submitted on April 24, 2018. This work is supported in part by the Lille University - Science and Technology, in part by the INRIA Research Center in Nancy Grand Est, in part by the Lebanese University – Azm Center for Biotechnology Research, and in part by the Université de Technologie et de Sciences Appliquées Libano-Française (ULF).

For readers' convenience and to make this paper self-contained, some parts have been reused (with permission) from Mohamad Daher's thesis [30].

*M. Daher is with the Lille University - Science and Technology, CRIStAL, UMR 9189, 59650 Villeneuve d'Ascq, France (e-mail: mohamad.daher@univ-lille1.fr).

J. Al Hage is with the Univerisity of Technology of Compiègne Heudiasyc UMR CNRS 72535 (e-mail: joelle.al-hage@hds.utc.fr).

M. El Badaoui El Najjar is with the Lille University - Science and Technology, CRIStAL, UMR 9189, 59650 Villeneuve d'Ascq, France (e-mail: maan.el-badaoui-el-najjar@univ-lille1.fr).

A. Diab is with Lebanese University, faculty of public health, Lebanon (e-mail: ahmaddiab@ul.edu.lb).

M. Khalil is with Lebanese University, faculty of engineering Azm research center in biotechnology, EDST, also with CRSI research center, faculty of engineering, Lebanon (e-mail: mohamad.khalil @ul.edu.lb).

F. Charpillet is with Université de Lorraine, CNRS, Inria, LORIA, F-54000 Nancy, France (e-mail: françois.charpillet@inria.fr).

reliability system by using data from multiple distributed sources. It is commonly used in different application domains, such as military applications, positioning systems and robotics [10]. Data fusion can be implemented using one of three theoretical frameworks: probability theory, belief theory, and possibilities theory. But, usually all of them share the following four steps (modeling, estimation, combination and decision) [11].

However, the most widely used data fusion methods employed in positioning originate in the fields of statistics, estimation and control. The major part of them is based on control system theory (observer based methods) and employs the laws of probability to compute a vector state from the measurements vectors. Furthermore, there are a number of alternatives to probabilistic methods that include the theory of evidence and interval methods.

Probabilistic data fusion methods are generally based on Bayes' rule for combining prior and observation information. Practically, this may be implemented in a number of ways: through the use of the Kalman filters (KF), Extended Kalman filters (EKF) and Unscented Kalman filter (UKF), through sequential Monte Carlo methods, or through the use of functional density estimates [12].

The informational filter (IF) uses the informational form of the state vector and the covariance matrix respectively named information vector (y) and informational matrix (Y). Similar to the KF, IF is broken down into two steps: a prediction step from the system evolution model and a correction step resulting from the use of the observations in the estimation procedure. It is more advantageous in the correction step than the KF and it allows a distributed and decentralized data fusion architecture [13]. Moreover, extended information filter (EIF) is used in case of nonlinear system [14].

A. State of the art on PLS

Several projects are developed around the world on the topic of PLS using multisource data fusion. In addition, there are many survey papers in the literature that present the latest indoor localization systems, e.g. [15,16,17]. However, the whole localization process is divided into two phases: signal measurement and position calculation. For the first phase, the three most widespread methods are the time based method, the angle based method, and the received signal strength based method. For the second phase, the trilateration and triangulation are the common used techniques, as well as the statistical techniques that could be employed to improve the solution accuracy by coping with measurement noise [18]. In the following, we present a brief overview of different existing PLS.

In 2004, the cooperation between Bluesoft and KidSpotter companies has successfully deployed the "WiFi Kid Tracker" system; a child tracking application within the LEGOLAND Park in Denmark. The approach is based on Bluesoft's AeroScout system that combines the RFID technology with the wireless sensor network technology [19]. In 2008, Woodman and Harle proposed a pedestrian localization system for indoor environments that uses foot-mounted inertial unit, a detailed building model and a particle filter [20]. In 2012, Shirehjini et al. proposed an indoor positioning system that provides two dimensional positioning and orientation information for mobile objects. The proposed system uses a low-range radio frequency identification technology and the results show that it performs better than similar existing systems in minimizing the average positioning inaccuracy [21]. In 2015, Kok et al. presented a 3D indoor positioning system that combines measurements from inertial sensors (accelerometers and gyroscopes) with time-of-arrival measurements from an ultra-wideband (UWB). Results show an excellent performance compared to the recent published systems [22]. In 2018, Mashuk et al. proposed a novel phone-based application of indoor positioning. It uses a particle filter that combines Bluetooth Low Energy (BLE) and Wi-Fi fingerprinting. The positioning algorithm utilizes a map matching and computes relative heading information from an orientation filter based on accelerometer and gyro data from the smart phone [23].

Despite the great progress made in recent years, there still is no standard for PLS, and there are a number of issues that need to be addressed such as (the impact of noise interference, the precision deficiency, the severe computational overhead, and the faulty sensors measurements) [1,18]. This work aims to offer a reliable, efficient and fault-tolerant system to locate and track people at home.

III. MATERIALS AND METHODS

The aim of this work is to develop a fault-tolerant PLS that localizes and tracks people in their home with a high accuracy. In this regard, we propose to use different and redundant sources of data (smart tiles, IMU and vision system) to allow a multisensory data fusion system with fault detection and exclusion (FDE). First, we have chosen to use the smart tiles and the vision system of the INRIA smart apartment as a non-intrusive system. However, in order to integrate these measurements in a recursive Bayesian filter, we have made the choice to use an IMU prediction model.

Thus, the main idea of the proposed method is the fusion between the simulated IMU sensor measurements (used in the frame of a pedometer model) and the load pressure sensors that give a representation of the load pressure distribution exerted by the person on the tiles. The pedometer model is used to predict the position of the person (named in the next by IMU prediction model), whereas the load pressure distribution is used to correct the predicted position (observation model for correction). This fusion aims to improve the localization integrity of the overall system, considering the fact that a person's movement is more erratic when compared, for instance, with a robot being tracked.

A. Sensors in use

The IMU intended to be used in this work to build the IMU prediction model is the SparkFun 9DoF Razor IMU M0[2]. It has three 3-axis sensors; an accelerometer, a gyroscope and a magnetometer; that offer the ability to sense linear acceleration, angular rotation velocity and magnetic field vectors. Moreover,

[2] https://www.sparkfun.com/products/14001

it is very small in size and installed in the waist of the person in such a way that does not disturb his/her normal movements.

The data reported by the IMU is fed into a processor that calculates the altitude, the velocity and the position of the person being tracked relative to a global reference frame. The angular rate collected from the gyroscope is used to calculate the angular position. This is fused with the gravity vector measured by the accelerometers in a KF to estimate the attitude. This attitude is used to transform acceleration measurements into an inertial reference frame where they are integrated once to get linear velocity, and twice to get global position. Thus, we can build an IMU prediction model to estimate the change in position over the time. Such system has a good accuracy in the short term, but it drifts as soon as the traveled distance becomes great. Therefore, the position of the person needs to be corrected periodically.

The load pressure sensors are of the brand SparkFun SEN-10245[3] that measure the load forces exerted on the floor. Each tile of the INRIA Nancy - Grand Est sensing floor is equipped with four load sensors concealed under the corners. Hence, the data reported by the load pressure sensors are used to correct the position based on the total weight of the person and its distribution on the four sensors.

In this way, EIF is used and it consists of the following two phases:

- The evolution phase (or prediction step) where an IMU prediction model resulting from the IMU sensor measurements are used to locate and track the trajectory followed by a subject in order to derive the evolution model,
- The correction phase (or update step) where the observations of the load pressure sensors values are used to correct the predicted position. A certain translation is made to convert from the local position (derived from the load pressure distributions on the tiles) to the global position (derived from the IMU prediction model).

B. Prediction step using an evolution model

The evolution equations of the EIF are described using the IMU prediction model. At instant *k*, the state vector of a person is considered to be the position (x, y) and the orientation (θ), namely the pose of the elder:

$$X_k = [x_k \; y_k \; \theta_k]^T \qquad (1)$$

The propagation model is a kinematic model resulted from the projection of the velocity vector on x axis and y axis as shown below:

$$X_{k+1/k} = X_{k/k} + A_k u_k + w_k = f(X_{k/k}, u_k) + w_k \qquad (2)$$

Where:

- $X_{k+1/k}$ is the estimate of *X* at instant *k + 1* given observations up to instant *k*,
- A_k is the input matrix,

$$A_k = \begin{bmatrix} cos\,\theta_k & 0 \\ sin\,\theta_k & 0 \\ 0 & 1 \end{bmatrix} \qquad (3)$$

- u_k is the input vector, it consists of the elementary displacement and rotation of the person; which is calculated from the IMU measurements: $u = [\Delta, \omega]^T$. Δ is calculated using the distance formula derived from the Pythagorean theorem; for two points (x_1,y_1) and (x_2,y_2), $\Delta = \sqrt[2]{(x_2-x_1)^2 + (y_2-y_1)^2}$, and ω is given by the gyroscope. In this work, Δ and ω are calculated using a camera-based sensing approach. By means of the mass center coordinates extracted from a simple RGB-D camera [24], we calculate Δ using the Pythagoras's theorem and ω using the arctangent function, i.e. $\omega = \arctan(\frac{y_2-y_1}{x_2-x_1})$.
- w_k is the process state noise modeled as Gaussian white noise with zero mean and covariance matrix Q_k.

$$X_{k+1\,/k} = \begin{bmatrix} x_{k+1} \\ y_{k+1} \\ \theta_{k+1} \end{bmatrix} = \begin{bmatrix} x_k \\ y_k \\ \theta_k \end{bmatrix} + \begin{bmatrix} \Delta_k \; cos\,\theta_k \\ \Delta_k \; sin\,\theta_k \\ w_k \end{bmatrix} + w_k = f(X_k, u_k) + w_k \qquad (4)$$

Since the model is nonlinear, the EIF is applied. Therefore, the Jacobian matrices $F_k = \left.\frac{\partial f}{\partial X}\right|_{X_{k/k}}$ and $B_k = \left.\frac{\partial f}{\partial u}\right|_{u_k}$ are computed:

$$F_k = \begin{bmatrix} 1 & 0 & -\Delta_k\, sin\,\theta_{k/k} \\ 0 & 1 & \Delta_k \cos\theta_{k/k} \\ 0 & 0 & 1 \end{bmatrix} \qquad (5)$$

$$B_k = \begin{bmatrix} \cos\theta_{k/k} & -\Delta_k \sin\theta_{k/k} \\ \sin\theta_{k/k} & \Delta_k \cos\theta_{k/k} \\ 0 & 1 \end{bmatrix} \qquad (6)$$

The covariance matrix corresponding to this evolution model is the following:

$$P_{k+1/k} = F_k P_{k/k} F_k^T + B_k (Q_u)_k B_k^T + Q_k \qquad (7)$$

Where:

- $(Q_u)_k$ is covariance matrix associated with the evolution model and the noise of measurements associated to the input vector u_k. It was defined regarding the datasheet of the SparkFun 9DoF Razor IMU M02.

Therefore, the informational matrix denoted $(Y_{k+1/k})$ and the information vector denoted $(y_{k+1/k})$ can be calculated as the following:

$$Y_{k+1/k} = P_{k+1/k}^{-1} \qquad (8)$$

$$y_{k+1/k} = Y_{k+1/k} X_{k+1/k} \qquad (9)$$

C. Correction step using an observation model

The IMU prediction model used for tracking people suffers from accumulated error driven from proprioceptive measurement errors, however small, are gathered over time. This leads to 'drift': a difference between where the system estimates the location of person and his/her actual real location. Thus, when a person presses on tiles, the weight is distributed

[3] https://www.sparkfun.com/products/10245.

over the pressure sensors under the tiles being exerted. These load pressures will be used to update the EIF that corrects the position of the person on a tile.

The fusion of the load pressure sensors observations with the data coming from the IMU prediction model is carried out using the IF [25]:

$$Y_{k/k} = Y_{k/k-1} + \sum_{i=1}^{N} I_i(k) \qquad (10)$$

$$y_{k/k} = y_{k/k-1} + \sum_{i=1}^{N} i_i(k) \qquad (11)$$

$$I_i(k) = H_{i,k}^T R_i^{-1}(k) H_{i,k} \qquad (12)$$

$$i_i(k) = H_{i,k}^T R_i^{-1}(k)\left[\left(W_{i,k} - \widehat{W}_{i,k}\right) + H_{i,k} X_{k/k-1}\right] \qquad (13)$$

Where:

- $I_i(k)$ and $i_i(k)$ are the informational contributions associated with the measurement of the i^{th} load pressure sensor,
- $\widehat{W}_{i,k}$ is the estimated load pressure amount of the i^{th} load pressure sensor,
- $W_{i,k}$ is the pressure measure received from the i^{th} load pressure sensor,
- $H_{i,k}$ is the i^{th} line of the matrix H_k that relates the parameters to be estimated to the observation measurements,
- N is the number of load pressure sensors under a tile,
- The noise associated with the load pressure sensors measurements is assumed to be uncorrelated. Similarly, each noise is assumed to be a Gaussian white noise of zero mean value and a covariance matrix $R_{i..}$

1) Load pressure estimation ($\widehat{W}_i$ calculation):

For a person having a weight (W) and a position coordinates (x_L, y_L) in a tile plan of dimension L (see Fig. 2), the estimated load pressures amount of the i^{th} load pressure sensor $(\widehat{W}_i)$ can be calculated using the Newton's laws assuming the following criteria:

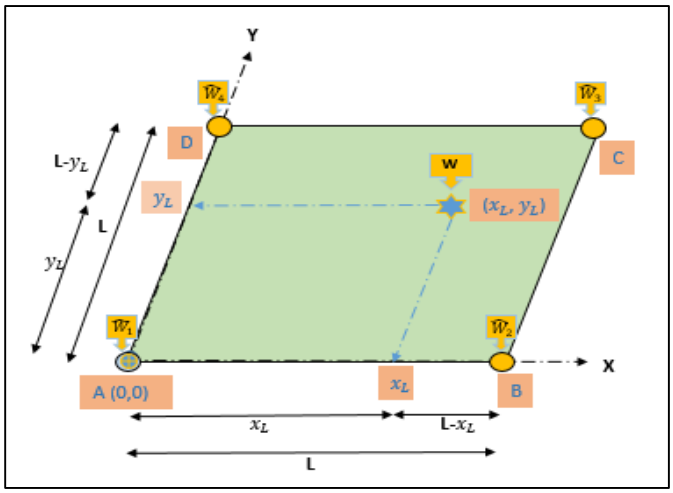

Fig. 2. A person having a weight of (W) and a position coordinates (x_L, y_L) in a tile plan of dimension L.

- The only points of contact between the tiles surface and the ground are the sensors,
- The ground and the sensors are considered infinitely rigid. Thus, the surface is not supposed to be deformed,
- The weight (W=mg) is normal; where m is the mass, and g is the gravitational field strength (about 9.81 m/s^2 on Earth); and the vertical forces "$\widehat{W}_i$" applied are perpendicular to its plane.
- The system is considered stable vertically and horizontally (using of pinned or fixed supports), then it becomes isostatic [26].

For a two-dimensional body and based on Newton's laws of motion, the equilibrium equations available are [27]:

- (i) $\sum \overrightarrow{F} = 0$: The vectorial sum of the forces acting on the body equals zero;
- (ii) $\sum \overrightarrow{M_A} = 0$: The sum of the moments (about an arbitrary point) of all forces equals zero.

$$(i): \sum \overrightarrow{F} = 0 \Rightarrow W - \widehat{W}_1 - \widehat{W}_2 - \widehat{W}_3 - \widehat{W}_4 = 0$$

$$\Rightarrow W = \widehat{W}_1 + \widehat{W}_2 + \widehat{W}_3 + \widehat{W}_4$$

As the tile is square shaped and the only points of contact between the tiles surface and the ground are the load sensors (A, B, C and D), thus the weight (W) can be divided into two parts such that $(\widehat{W}_1 + \widehat{W}_4)$ on [AD] and $(\widehat{W}_2 + \widehat{W}_3)$ on [BC] (see Fig. 3).

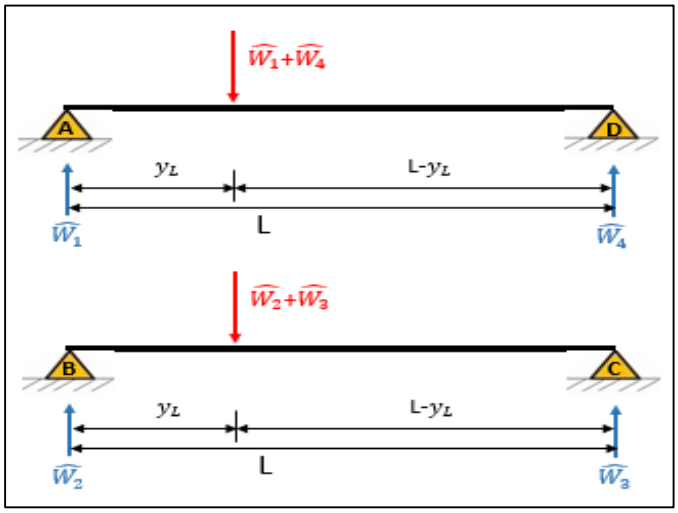

Fig. 3. The weight (W) is divided into two parts: $(\widehat{W}_1 + \widehat{W}_4)$ on [AD] (top) and $(\widehat{W}_2 + \widehat{W}_3)$ on [BC] (down).

Where:

$$\begin{cases} \widehat{W}_1 + \widehat{W}_4 = \dfrac{W \times (L - x_L)}{L} \\ \widehat{W}_2 + \widehat{W}_3 = \dfrac{W \times x_L}{L} \end{cases}$$

$$(ii): \sum \overrightarrow{M_A} = 0 \Rightarrow -\widehat{W}_1 \times 0 + (\widehat{W}_1 + \widehat{W}_4) \times y_L - \widehat{W}_4 \times L$$

$$= 0 \Rightarrow \widehat{W}_4 = \frac{W \times (L - x_L) y_L}{L^2}$$

$$\widehat{W}_1 = \frac{W \times (L - x_L)}{L} - \widehat{W}_4 \Rightarrow \widehat{W}_1 = \frac{W \times (L - x_L)(L - y_L)}{L^2}$$

$$\sum \overrightarrow{M_B} = 0 \Rightarrow -\widehat{W_2} \times 0 + (\widehat{W_2} + \widehat{W_3}) \times y_L - \widehat{W_3} \times L = 0$$

$$\Rightarrow \widehat{W_3} = \frac{W \times x_L y_L}{L^2}$$

$$\widehat{W_2} = \frac{W \times x_L}{L} - \widehat{W_3} \Rightarrow \widehat{W_2} = \frac{W \times x_L (L - y_L)}{L^2}$$

Thus,

$$\widehat{W} = \begin{bmatrix} \widehat{W_1} \\ \widehat{W_2} \\ \widehat{W_3} \\ \widehat{W_4} \end{bmatrix} = \begin{bmatrix} \frac{W \times (L - x_L)(L - y_L)}{L^2} \\ \frac{W \times x_L (L - y_L)}{L^2} \\ \frac{W \times x_L y_L}{L^2} \\ \frac{W \times (L - x_L) y_L}{L^2} \end{bmatrix}$$

Since the platform has a rectangular form with (nxm) tiles (see Fig.2), we can calculate the position (x, y) using the following equations:

$$\begin{cases} x_L = x - [(i-1)\%n] = x - k_1 \\ y_L = y - (i \; div \; n) = y - k_2 \end{cases}$$

Where:

- $\%$ operation (modulo) is the remainder of the Euclidean division,
- div operation is the Euclidean division,
- i is the identifier for the tile,
- $x_L \; and \; y_L$ are the local position coordinates (the origin is at the Bottom-Left of current tile having the identifier equal to i),
- $x \; and \; y$ are the position coordinates of a person in the global frame where the origin (0,0) is at the bottom left corner of the cartography of the platform (see Fig. 4).

Fig. 4. The position coordinates of a person in the global frame of the platform plan represented on the cartography of the tiles with their identifiers. Note that, the red dots in the corners of tiles indicate the positions of the load pressure sensors.

Therefore,

$$\widehat{W} = \begin{bmatrix} \widehat{W_1} \\ \widehat{W_2} \\ \widehat{W_3} \\ \widehat{W_4} \end{bmatrix} = \begin{bmatrix} \frac{W \times (L - x + k_1)(L - y + k_2)}{L^2} \\ \frac{W \times (x - k_1)(L - y + k_2)}{L^2} \\ \frac{W \times (x - k_1)(y - k_2)}{L^2} \\ \frac{W \times (L - x + k_1)(y - k_2)}{L^2} \end{bmatrix} = h(X_k) \qquad (14)$$

2) H_k Calculation:

As the observation model is non-linear, its linearization around the predicted pose yields the Jacobian: $H_k = \left.\frac{\partial h}{\partial X}\right|_{X = X_{k/k-1}} \Rightarrow H_k = \left[\frac{\partial W_i}{\partial X_k}\right] = [\frac{\partial W_1}{\partial X_k} \; \frac{\partial W_2}{\partial X_k} \; \frac{\partial W_3}{\partial X_k} \; \frac{\partial W_4}{\partial X_k}]^T$

Where:

$$\frac{\partial W_i}{\partial X_k} = \begin{bmatrix} \frac{\partial W_i}{\partial x} & \frac{\partial W_i}{\partial y} & \frac{\partial W_i}{\partial \theta} \end{bmatrix}$$

$$\Rightarrow H_k = \begin{bmatrix} \frac{\partial W_1}{\partial x} & \frac{\partial W_1}{\partial y} & \frac{\partial W_1}{\partial \theta} \\ \frac{\partial W_2}{\partial x} & \frac{\partial W_2}{\partial y} & \frac{\partial W_2}{\partial \theta} \\ \frac{\partial W_3}{\partial x} & \frac{\partial W_3}{\partial y} & \frac{\partial W_3}{\partial \theta} \\ \frac{\partial W_4}{\partial x} & \frac{\partial W_4}{\partial y} & \frac{\partial W_4}{\partial \theta} \end{bmatrix}_{k/k-1}$$

$$\begin{cases} \frac{\partial W_1}{\partial x} = \frac{-W}{L^2}(L - y + k_2) \\ \frac{\partial W_1}{\partial y} = \frac{-W}{L^2}(L - x + k_1) \\ \frac{\partial W_1}{\partial \theta} = 0 \end{cases} \quad \begin{cases} \frac{\partial W_2}{\partial x} = \frac{W}{L^2}(L - y + k_2) \\ \frac{\partial W_2}{\partial y} = \frac{-W}{L^2}(x - k_1) \\ \frac{\partial W_2}{\partial \theta} = 0 \end{cases}$$

$$\begin{cases} \frac{\partial W_3}{\partial x} = \frac{W}{L^2}(y - k_2) \\ \frac{\partial W_3}{\partial y} = \frac{W}{L^2}(x - k_1) \\ \frac{\partial W_3}{\partial \theta} = 0 \end{cases} \quad \begin{cases} \frac{\partial W_4}{\partial x} = \frac{-W}{L^2}(y - k_2) \\ \frac{\partial W_4}{\partial y} = \frac{W}{L^2}(L - x + k_1) \\ \frac{\partial W_4}{\partial \theta} = 0 \end{cases}$$

Then,

$$H_k = \begin{bmatrix} \frac{-W(L - y + k_2)}{L^2} & \frac{-W(L - x + k_1)}{L^2} & 0 \\ \frac{W(L - y + k_2)}{L^2} & \frac{-W(x - k_1)}{L^2} & 0 \\ \frac{W(y - k_2)}{L^2} & \frac{W(x - k_1)}{L^2} & 0 \\ \frac{-W(y - k_2)}{L^2} & \frac{W(L - x + k_1)}{L^2} & 0 \end{bmatrix}_{k/k-1} \qquad (15)$$

D. Fault detection and exclusion using informational framework

The FDE aims to enable systems to continue operating in the presence of some erroneous measurements.

1) Fault detection

In this section, we propose a method for detection and exclusion of faulty sensors based on the use of *KLD* for residual synthetizing. The *KLD* permits to compute the divergence between two probability density functions (pdf) [7]. Recall that the *KLD* from a pdf q to a pdf p is defined as:

$$KL(p\|q) = \int p(X) \log\left(\frac{p(X)}{q(X)}\right) dX \qquad (16)$$

The *KLD* can be written in the form:

$$KLD(f(x)\|g(x)) = \frac{1}{2}\left[trace\,(P_2^{-1}P_1) + \text{Log}\left(det\left(\frac{P_2}{P_1}\right)\right) - d + (\mu_1 - \mu_2)^T P_2^{-1}(\mu_1 - \mu_2)\right] \qquad (17)$$

Where:

Log represents the natural logarithm, and ($P1$, $\mu 1$), ($P2$, $\mu 2$) are the covariance matrices and the means of two Gaussian distributions $f(x)$ and $g(x)$.

This informational metric can be considered as the expected Log Likelihood Ratio (LLR). It takes in consideration the Mahalanobis distance and the Bergmann divergence that assess the orientation and the compactness of the measurements distributions represented respectively by the trace and the determinant of their covariance matrices [7,28].

The *KLD* between the data distribution obtained in the predicted step of the EIF ($g(k/k-1)$) and the distribution obtained in the corrected step ($g(k/k)$) is called the Global Kullback-Leibler Divergence (*GKLD*) [7,28,29], and it has the following form:

$$GKLD = KLD(g(k/k-1)\|g(k/k)) = \frac{1}{2}\left[trace\left(Y_{k/k}\ Y_{k/k-1}^{-1}\right) + \text{Log}\frac{|Y_{k/k-1}|}{|Y_{k/k}|} - M + \left(X_{k/k} - X_{k/k-1}\right)^T Y_{k/k}\left(X_{k/k} - X_{k/k-1}\right)\right] \qquad (18)$$

Where M is the dimension of the state vector.

This equation takes the form of a residual test to detect the presence of the faulty measurements in the load pressure sensors as well as in the IMU measurements.

The *GKLD* measures the divergence between the posterior and the prior distributions obtained from the informational filter. If the *GKLD* exceeds a predetermined threshold, this implies a divergence of the estimate obtained after incorporating observations from the load pressure sensors with respect to the estimate obtained from the IMU prediction model.

Note that the threshold is preset by tuning based on the determination of the false alarm probability and the probability of detection. Actually, the threshold value is determined heuristically.

2) Fault exclusion

After a faulty measurement detection, the erroneous measurement must be identified in order to be excluded from the fusion procedure. For that reason, N (EIF_j) filters are designed in such way that each filter uses the measurements of the corresponding load pressure sensor j. The statistical test associated with each filter is obtained from the calculation of the KL divergence between the corrected state using the j^{th} load sensor measurements and the predicted state using the IMU prediction model. This residual is named the Partial Kullback-Leibler Divergence (*PKLD*) and can be represented by the equation below:

$$PKLD_{j,k} = \frac{1}{2}trace\left(Y_{j,k/k}\ Y_{k/k-1}^{-1}\right) + \frac{1}{2}Log\frac{|Y_{k/k-1}|}{|Y_{j,k/k}|} - \frac{1}{2}M + \frac{1}{2}\left(X_{j,k/k} - X_{k/k-1}\right)^T Y_{j,k/k}\left(X_{j,k/k} - X_{k/k-1}\right) \qquad (19)$$

Where:

$$Y_{j,k/k} = Y_{k/k-1} + I_j(k) \qquad (20)$$

$$y_{j,k/k} = y_{k/k-1} + i_j(k) \qquad (21)$$

$$X_{j,k/k} = \left(Y_{j,k/k}\right)^{-1} y_{j,k/k} \qquad (22)$$

In the case where a $PKLD_j$ surpasses a predefined threshold, yet the j^{th} load pressure sensor may be then faulty, and consequently it will be excluded from the fusion process. A significant increasing in all *PKLDj* implies that the erroneous measurements come probably from the IMU, so the faulty IMU prediction model measurements will be excluded from the fusion procedure. While a significant increasing in at most three of the four *PKLDj* implies that the corresponding sensors faulty, and then the four load pressure sensors of the same tile are excluded from the fusion procedure.

The "Fig. 5" shows the procedure for fault detection and exclusion using the filter bank with the corresponding residues.

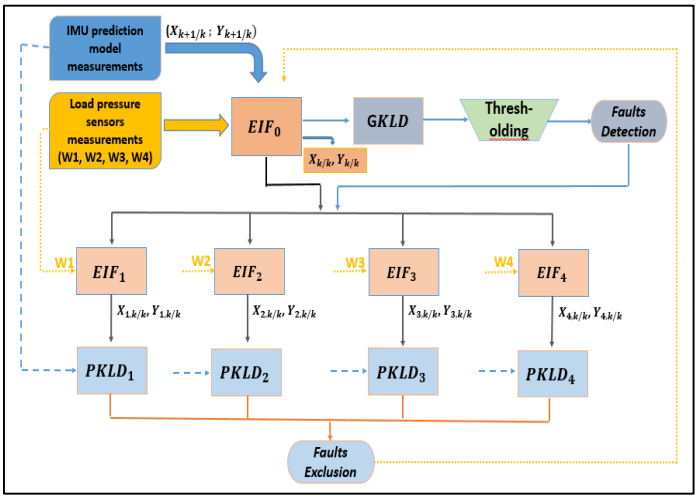

Fig. 5. The faulty measurements detection and exclusion architecture.

IV. EXPERIMENTS

In order to test the performance of the proposed approach, experiments with simulated IMU measurements and real load pressure data are realized. Six persons of different ages start moving separately on the sensing floor and performing some ADLs such as walking, standing, sitting, lying down, and also falling down. Several experiments have been realized, but only one experiment is presented with details here. The performance of the other experiments is also shown at the end of this section.

For the following scenario, a person is entering from the tile 7, starts walking on tiles, sits on a chair posed on tile 5 and tile 6, stands up and then walks with sudden turn and random movement and finally exits from the tile 18. In addition, he walked on defected tiles offering faulty measurements in order to test the ability of detecting them and thereafter excluding them from the fusion procedure.

This scenario is shown in the "Fig. 6" where the real trajectory of the person (named in the next by reference trajectory) has been drawn in yellow color.

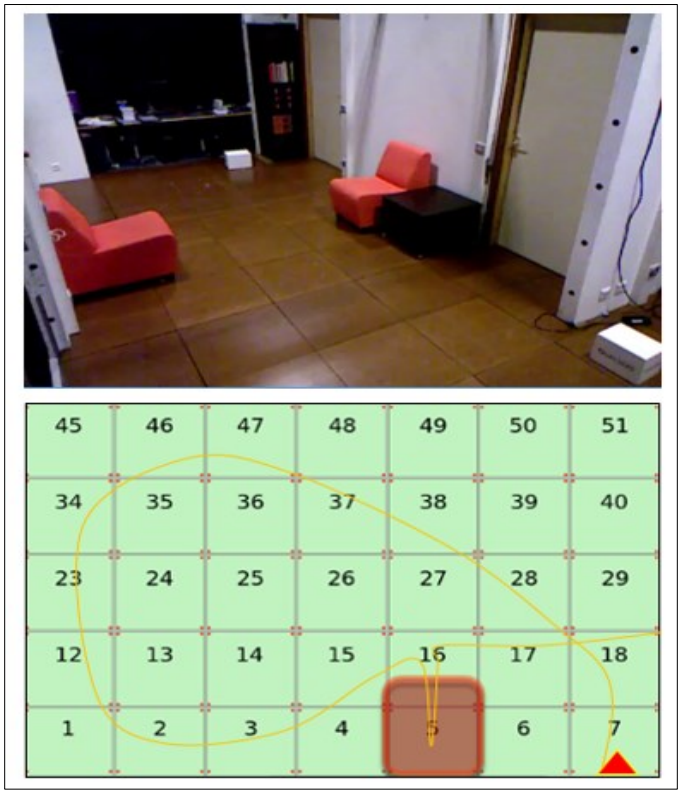

Fig. 6. The real platform (top) and the cartography of the tiles with their identifiers and the reference trajectory in yellow color (down).

V. RESULTS AND DISCUSSIONS

For this scenario, the "Fig. 7" shows the predicted trajectory derived from the IMU prediction model (in blue color) compared to the reference trajectory (in yellow color). One can see that the IMU prediction model trajectory is not very accurate especially on the tiles 7, 18, 35, 24, 23, 16, 17 and 18.

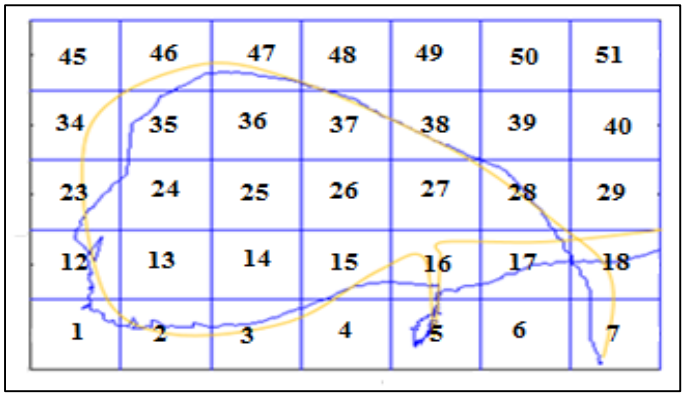

Fig. 7. The estimated trajectory derived from the IMU prediction model compared to the reference trajectory.

After the fusion between the IMU prediction model and the load pressure sensors' measurements, one can remark that the estimated trajectory becomes closer to the reference trajectory and particularly after FDE. The "Fig. 8" shows the trajectory before FDE (in dotted red color) compared to the reference trajectory (in yellow color). On the other hand, the "Fig. 9" shows the same trajectory after FDE.

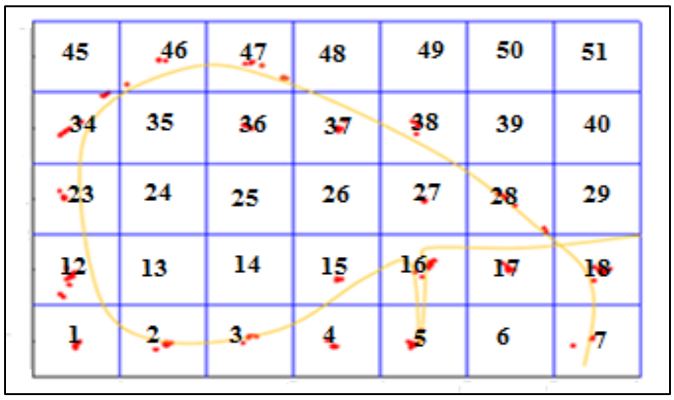

Fig. 8. The estimated trajectory before FDE of a person after data fusion between the IMU and the load pressure sensors' measurements (in dotted red color) compared to the reference trajectory (in yellow color).

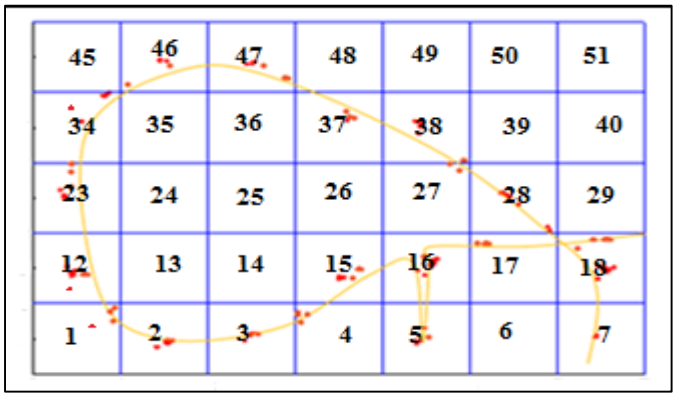

Fig. 9. The estimated trajectory after FDE.

As it is mentioned in the section III.D.1, faults are detected using the *GKLD*. This informational quantity measures the divergence between the IMU prediction model and the corrected load pressure sensors estimates. The results, which are illustrated in the "Fig. 10", show several jumps above the predefined threshold indicating the presence of erroneous measurements.

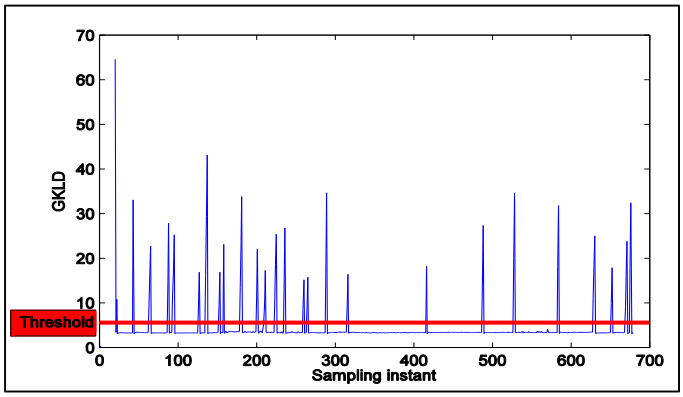

Fig. 10. The *GKLD* used for fault detection.

As an example of FD, the "Fig. 11" shows a zoom in on a certain part of the *GKLD* for the observed jumps of $k = 626$ to $k = 632$.

One can see that from $k = 627$ to 631 the *GKLD* is above the threshold declaring fault measurements detection.

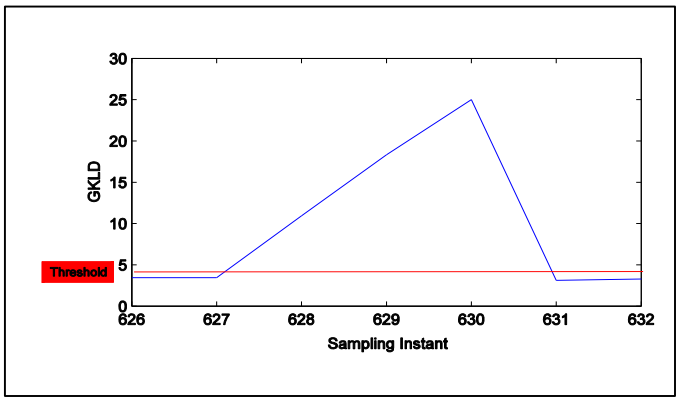

Fig. 11. The jump in the *GKLD* representing a fault detection.

Once erroneous measurements are detected using the *GKLD*, the faulty sensors must be excluded from the fusion procedure.

A significant increasing in all *PKLDj* implies that the four load pressures sensors give erroneous measurements, and here we assume that the error comes probably from the IMU measurements. Consequently, the faulty IMU prediction model measurements will be excluded from the fusion procedure. Otherwise, the tile measurements are excluded from the fusion procedure. The "Fig. 12" shows the residues $PKLD_j$ used for the exclusion of faulty measurements.

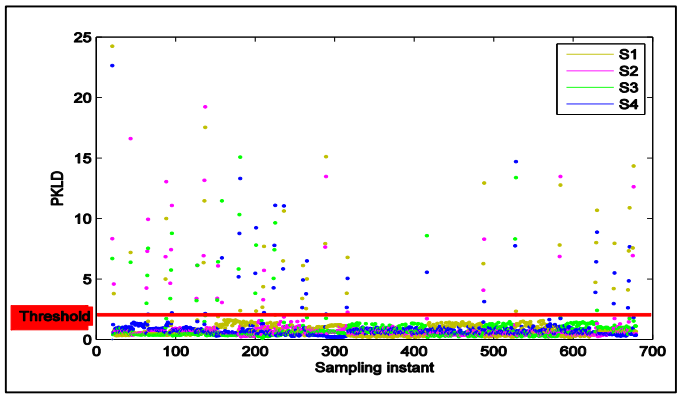

Fig. 12. The residues *PKLD* used for the exclusion of faulty measurements.

The *PKLDi* analysis for a sampling instant $k = 627$ to 631 provided in the "Fig. 13" shows that the $PKLD_3$ has a jump at instant $k = 627$, whereas $PKLD_1$, $PKLD_2$ and $PKLD_4$ remain below the threshold. This result indicates that one of the four load pressures sensors (noticed the third sensor) is defected, involving the necessity of excluding the corresponding tile from the fusion procedure during this interval.

Similarly, jumps at $PKLD_1$ and $PKLD_4$ indicate that two load pressure sensors are defected, then the corresponding tile should be excluded from the fusion procedure at $k = 628$.

At $k = 629$, the $PKLD_1$, $PKLD_3$ and $PKLD_4$ have jumps indicating the defect of three load pressure sensors measurements, then the corresponding tile must be excluded from the fusion procedure.

At $k = 630$, the $PKLD_1$, $PKLD_2$, $PKLD_3$ and $PKLD_4$ have jumps indicating the defect of the four load pressure sensors measurements. Indeed, in case where all pressure sensors give estimates that diverge from the predicted ones obtained from the IMU, we consider that the IMU measurement is more likely to be erroneous.

Consequently, the proposed method is capable of handling the FDE in a relevant manner.

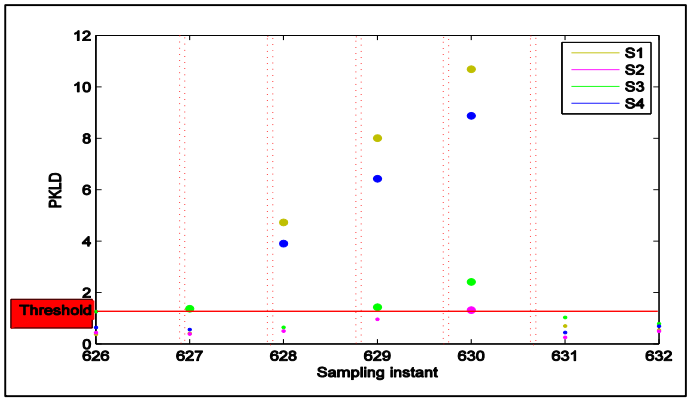

Fig. 13. Example of different faults exclusion using *PKLD*.

To evaluate the performance of the proposed method, we calculate the localization error ratio (LER). LER is calculated by dividing the number of erroneous localization points over the number of all localization points. Thus, we calculate the difference between the reference trajectory and the three following cases. (1): the estimated trajectory derived from the IMU prediction model, (2): the estimated trajectory after data fusion between the IMU and the load pressure sensors' measurements without FDE, and (3): the estimated trajectory after data fusion and with FDE. In this statistical study, the estimated position is considered as an erroneous position if the distance between the reference trajectory and the estimated one is greater than 15 cm at each discretized point.

Five different experiments with different subjects including the previous detailed experiment (Exp. 1) were experienced to show the performance of the proposed method. "Table 1" shows the LER for the three previous cases.

TABLE 1: LER OF THE THREE PREVIOUS CASES

Experiments	IMU LER	LER after data fusion and without FDE	LER after data fusion and with FDE

Exp. 1	37.3%	16.2%	5.5%
Exp. 2	29.8%	15.5%	7.3%
Exp. 3	33%	18.3%	9%
Exp. 4	34.6%	20%	7%
Exp. 5	40.4%	22.1%	9.7%

Thus, one can remark that the proposed data fusion method between the IMU and the load pressures sensors can reduce the average IMU LER from 35% to 18.4% (i.e. ~47.4%). Furthermore, by excluding the erroneous measurements driven from the IMU and the load pressure sensors, the LER decreases from 35% to 7.7% (i.e. ~78%).

VI. CONCLUSION

This paper aims to show the performance of the proposed approach on PLS application in an indoor environment using a multi-sensor data fusion between IMU and load pressure sensors with FDE. The FDE step is formulated in an informational framework using the *KLD* between the predicted and the corrected distributions of the IF. The residual tests based on the *KLD* have many advantages as they take into account the Bregman matrix divergence between covariance matrices as well as the Mahalanobis distance. The *GKLD* test detects the presence of faulty measurements from both the load pressure sensors and the IMU.

First, we presented a brief overview of state-of-the-art localization technologies for tracking individuals in indoor environments, as well as some existing projects.

Second, a description of the IMU sensor has been exposed and an IMU prediction model has been proposed to estimate the personal trajectory.

Third, the fusion between the load pressure sensors and the IMU sensor measurements using EIF is detailed. In this regard, IF is used in the correction step for its advantages over KF when used in a fault tolerant formalism.

Fourth, we described a phase of erroneous measurements detection and exclusion using residues based on *KLD*.

Finally, experiment studies of the proposed framework are presented in order to show the performance of the proposed approach.

As perspectives, we will proceed this work to track multiple persons simultaneously as well as developing an adaptive threshold optimization using the information theory metrics.

REFERENCES

[1] https://en.wikipedia.org/wiki/Positioning_system. Accessed on April 20, 2017.

[2] D. Dardari, P.Closas, and P.M. Djurić. "Indoor tracking: Theory, methods, and technologies." *IEEE Transactions on Vehicular Technology* 64, no. 4 (2015): 1263-1278.

[3] H. Huang, and G. Gartner. "A survey of mobile indoor navigation systems." *Cartography in Central and Eastern Europe* (2010): 305-319.

[4] Y. Gu, A. Lo, and I. Niemegeers. "A survey of indoor positioning systems for wireless personal networks." *IEEE Communications surveys & tutorials* 11, no. 1 (2009): 13-32.

[5] M. Daher, M. El Badaoui El Najjar, A. Diab, M. Khalil, and F. Charpillet. " Elder Tracking and Fall Detection System using Smart Tiles". *IEEE Sensors Journal, vol. PP* 99 (2016): 1-1.

[6] N. Pepin, O. Simonin, and F. Charpillet, "Intelligent Tiles-Putting Situated Multi-Agents Models in Real World," ICAART. 2009.

[7] J. Al Hage. "Fusion de données tolérante aux défaillances: application à la surveillance de l'intégrité d'un système de localisation." PhD diss., Lille 1, 2016.

[8] A.M. Martins, A.D. Neto, J.D. Melo. "Comparison between mahalanobis distance and kullback-leibler divergence in clustering analysis." *Wseas Transactions on Systems* 3 (2004): 501-505.

[9] F. Pérez-Cruz. Kullback–Leibler divergence estimation of continuous distri- butions, in: Inf. Theory 20 08 ISIT 20 08 IEEE Int. Symp. On, IEEE, 2008, pp. 1666–1670.

[10] R. R. Brooks, and S. S. Iyengar. Multi-sensor fusion: fundamentals and applications with software. Prentice-Hall, Inc., 1998.

[11] A. Martin, 2005. La fusion d'informations. Polycopié de cours ENSIETA-Réf, 1484, p.117.

[12] D. Hall, and J. Llinas, eds. *Multisensor data fusion*. CRC press, 2001.

[13] M. Bozorg, E. M. Nebot, and H. F. Durrant-Whyte. "A decentralised navigation architecture." In *Robotics and Automation, 1998. Proceedings. 1998 IEEE International Conference on*, vol. 4, pp. 3413-3418. IEEE, 1998.

[14] T. Kobayashi, and D.L. Simon. "Application of a bank of Kalman filters for aircraft engine fault diagnostics." *ASME Paper No. GT2003-38550*(2003).

[15] G. Deak, K. Curran, and J. Condell. "A survey of active and passive indoor localization systems." *Computer Communications* 35, no. 16 (2012): 1939-1954.

[16] I. Amundson, and X.D. Koutsoukos. "A survey on localization for mobile wireless sensor networks." In *Mobile entity localization and tracking in GPS-less environnments*, pp. 235-254. Springer, Berlin, Heidelberg, 2009.

[17] H. Lui, H. Darabi, P. Banerjee, J. Liu. "Survey of wireless indoor positioning techniques and systems." *IEEE Transactions on Systems, Man, and Cybernetics, Part C (Applications and Reviews)* 37, no. 6 (2007): 1067-1080.

[18] D. Zhang, F. Xia, Z. Yang, L. Yao, and W. Zhao. "Localization technologies for indoor human tracking." In *Future Information Technology (FutureTech), 2010 5th International Conference on*, pp. 1-6. IEEE, 2010.

[19] http://www.mobiletechnews.com/info/2004/04/27/011106.html. Accessed on May 15, 2017.

[20] O. Woodman, and R. Harle. "Pedestrian localisation for indoor environments." In *Proceedings of the 10th international conference on Ubiquitous computing*, pp. 114-123. ACM, 2008.

[21] A. N. Shirehjini, A. Yassine, and S. Shirmohammadi. "An RFID-based position and orientation measurement system for mobile objects in intelligent environments." *IEEE Transactions on Instrumentation and Measurement* 61, no. 6 (2012): 1664-1675.

[22] M. Kok, J. D. Hol, and T. B. Schön. "Indoor positioning using ultrawideband and inertial measurements." *IEEE Transactions on Vehicular Technology* 64, no. 4 (2015): 1293-1303.

[23] M.S. Mashuk, J. Pinchin, P. Siebers, and T. Moore. "A smart phone based multi-floor indoor positioning system for occupancy detection." In *Position, Location and Navigation Symposium (PLANS), 2018 IEEE/ION*, pp. 216-227. IEEE, 2018.

[24] A. Dubois, and F. Charpillet. "A gait analysis method based on a depth camera for fall prevention." In Engineering in Medicine and Biology Society (EMBC), 2014 36th Annual International Conference of the IEEE, pp. 4515-4518. IEEE, 2014.

[25] S. Thrun, Y. Liu, D. Koller, A. Y. Ng, Z. Ghahramani, and H. Durrant-Whyte. "Simultaneous localization and mapping with sparse extended information filters." *The International Journal of Robotics Research* 23, no. 7-8 (2004): 693-716.

[26] http://www.mechanicalbooster.com/2016/11/types-of-support.html. Accessed on Feb 05, 2017.

[27] https://en.wikipedia.org/wiki/Statically_indeterminate. Accessed on Feb 05, 2017.

[28] J. Al Hage, M.E. El Najjar, and D. Pomorski. "Multi-sensor fusion approach with fault detection and exclusion based on the Kullback–Leibler Divergence: Application on collaborative multi-robot system." *Information Fusion* 37 (2017): 61-76.

[29] H. Durrant-Whyte and T. C. Henderson. "Multisensor data fusion." In *Springer Handbook of Robotics*, pp. 585-610. Springer Berlin Heidelberg, 2008.

[30] Daher, M. "High Integrity Personal Tracking Using Fault Tolerant Multi-Sensor Data Fusion." PhD diss., Université de Lille 1, Sciences et Technologies; CRIStAL UMR 9189, 2017.

Mohamad Daher received the teaching diploma degree in applied mathematics, option informatics from the Lebanese University, Tripoli-Lebanon, in 2002, and the Master's degree in computer science, option networking and communications from the University of Balamand, Al Kurah-Lebanon, in 2004. In 2017, he received his Ph.D. degree in informatics and automatic from Lille University - Science and Technology, Lille, France.

He joined the Université de Technologie et de Sciences Appliquées Libano-Française (ULF) in 2005 as instructor and also the Lebanese University in 2011. Since 2010, he is the head of the computer science department and an academic advisor at the ULF. His current research is focused on Multi-sensor fusion, Fault tolerant systems, activity recognition, and assistive living systems.

Joelle Al Hage received the engineer degree in electrical and electronic engineering (specialty control and industrial computing) and the master degree in Reliability, Identification and Diagnosis from the Lebanese university in 2013. She received the Ph.D. degree in automatic and computer science from university of Lille, France in 2016. Since October 2017, she's a CNRS young researcher at SIVALab laboratory (shared laboratory between Renault/Heudiasyc/CNRS) of the Université de Technologie de Compiègne, France.

Her research is focused on the multi-sensor data fusion with fault tolerance aspect and on the integrity of localization and perception methods for autonomous vehicles.

Maan El Badaoui El Najjar received his Engineer Diploma and his Master of Science degrees in control system from the INP Grenoble - France respectively in 1999 and 2000. He received the Ph.D. degree in Perception and Control Systems from the University of Technology of Compiegne in 2003. In November 2011, he obtained the Habilitation à Diriger des Recherches from the University of Lille.

He joined the University of Lille in 2005 as a permanent associate Professor. Since 2014, he is Full Professor at the same University. He is also with the CRIStAL Laboratory UMR 9189, a joint research unit between CNRS, University of Lille and Ecole Centrale de Lille. He is also the head of the DiCOT Team "Diagnostic, Control and Observation for fault Tolerant Systems" of the CRIStAL Laboratory**.**

The research of Prof. El Badaoui El Najjar is focused on Multi-sensor fusion, Fault tolerant systems, Multi-robots systems and GNSS.

Ahmad Diab received the degree in Biomedical Engineer from the Islamic University of Lebanon, Khalde, Lebanon, in 2010, and the M.Sc. degree in Medical and Industrial Processing and System from the Lebanese University, Tripoli, Lebanon, in 2011. Also he received his Ph.D. degree from the University of Technology of Compiègne, Compiègne, France and Reykjavik University, Reykjavik, Iceland in 2014.

He is currently an associate Professor in the faculty of public health, Lebanese University.

Mohamad Ali Khalil received an engineering degree in electrical and electricity from the Lebanese University, faculty of engineering, Tripoli, Lebanon in 1995. He received the DEA in biomedical engineering from the University of Technology of Compiegne (UTC) in France in 1996. He received his Ph.D. from the University of Technology of Troyes in France in 1999. He received the Habilitation à Diriger des Recherches from UTC in 2006.

He is currently teacher and researcher at Lebanese University, faculty of engineering. From 2009, he is director of the Azm center for research in biotechnology at the doctoral school of sciences and technology at the Lebanese university. He is the chair of the EMBS chapter in Lebanon and also the chair of ICABME international Conference.

The interests of Prof. Khalil are the signal and image processing problems: detection, classification, analysis, representation and modeling of non-stationary signals, with application to biomedical signals and images.

François Charpillet received his engineering degree from École Nationale Supérieure d'Électricité et de Mécanique (ENSEM) of the National Polytechnic Institute of Lorraine (INPL) in 1982. He received the M.S. and Ph.D. degree in computer science from Henri Poincaré University, Nancy, France, in 1982 and 1985 respectively. After a period as an engineer at Direction des Constructions Navales (DCN) in Paris, he joined the University of Lorraine and LORIA Lab as an assistant professor in 1987. In 1988, he got a research position at Inria Nancy - Grand-Est Research Center.

Prof. Charpillet is today Director of Research at Inria. From 1998 to 2014, he has been the leader of LORIA team MAIA, which was a joint research group with Inria, CNRS and University of Lorraine. Since 2015, he is the scientific leader of the new Inria team Larsen, focusing on Long Term Robotics, Human-robot interaction and Active and Distributed sensing. His current research interests concern multi-robot cooperation, human-robot- environment interaction, activity recognition, active sensing and ambient Intelligence.